https://doi.org/10.5194/wes-2021-9
Preprint. Discussion started: 1 March 2021

eawe european academy of wind energy
Open Access WIND ENERGY SCIENCE DISCUSSIONS

Model-based design of a wave-feedforward control strategy in floating wind turbines

Alessandro Fontanella[1], Mees Al[2], Jan-Willem van Wingerden[3], and Marco Belloli[1]

[1]Mechanical Engineering Department, Politecnico di Milano, Milano, Via La Masa 1, 20156, Italy.
[2]Sowento GmbH, Donizettistraat 1A, 70195 Stuttgart, Germany.
[3]Delft Center for Systems and Control, Delft University of Technology, Delft, 2628 CD, The Netherlands.

Correspondence: Alessandro Fontanella (alessandro.fontanella@polimi.it)

Abstract. Floating wind turbines rely on feedback-only control strategies to mitigate the effects of wave excitation. Improved power generation and lower fatigue loads can be achieved by including information about the incoming waves into the wind turbine controller. In this paper, a wave-feedforward control strategy is developed and implemented in a 10MW floating wind turbine. A linear model of the floating wind turbine is established and utilized to show how wave excitation affects the wind turbine rotor speed output, and that collective-pitch is an effective control input to reject the wave disturbance. Based on the inversion of the same model, a feedforward controller is designed, and its performance is examined by means of linear analysis. A gain-scheduling algorithm is proposed to adapt the feedforward action as the wind speed changes. Non-linear time-domain simulations prove that the proposed feedforward control strategy is an effective way of reducing rotor speed oscillations and structural fatigue loads caused by waves.

1 Introduction

Floating offshore wind turbines (FOWTs) are currently operated without any real-time information about ocean conditions. Industry-standard controllers are feedback-only: the wind turbine controller reacts to the external disturbance of wind and waves as it occur. One possibility to improve the current floating wind technology is to include information about the marine environment into the wind turbine controller and to design new control logics based on it.

Concerning wind turbulence, feedforward control has recently drawn the attention of the research community, as it can effectively reduce the fatigue loads and improve power production. Research has been mainly driven by the improvements in the LIDAR (light detection and ranging) technology that enables the measurement of the wind field upstream the wind turbine. The potential of LIDAR-assisted control were investigated in Harris et al. (2006). Since then, several control logics were developed Laks et al.; Dunne et al. (a,b,c); Schlipf et al. (2013). Very few are the studies about LIDAR-assisted FF control in floating wind turbines: in Schlipf et al. (2015), a collective-pitch FF controller is designed in order to reduce the rotor speed oscillations caused by turbulence. The LIDAR moves with the floating wind turbine and measurements need to be corrected for that. The proposed FB-FF controller, that keeps into account the above-mentioned movement of the LIDAR, can reduce power and rotor speed fluctuations up to 80% and tower, rotor-shaft, and blades fatigue loads of 20%, 7% and 9%, respectively.

https://doi.org/10.5194/wes-2021-9
Preprint. Discussion started: 1 March 2021

eawe european academy of wind energy
Open Access WIND ENERGY SCIENCE DISCUSSIONS

Applying the wind-feedforward concept to waves is an attractive perspective, as the wave disturbance is responsible of a large fraction of the fatigue loads experienced by a floating wind turbine. However, the idea is still largely unexplored. In Yu Ma and Paul D. Sclavounos and John Cross-Whiter and Dhiraj Arora (2018) two algorithms for real-time forecasting of wave forces are developed and validated. Based on the predicted wave forces, a finite-horizon LQR controller is designed and applied to a TLP-FOWT to minimize the tower-base fore-aft bending moment, achieving mixed results. In Al et al. (2020) an inversion-based feedforward control strategy is introduced, showing it is an effective way of reducing wave-induced rotor speed oscillations.

The present paper further develops the concept of wave-feedforward exploiting the tools of model-based control. The wave-feedforward control strategy is enabled by the use of an integrated model of the floating wind turbine that captures all its relevant physics. Hence, this work proves the effectiveness of multidisciplinary analysis as a mean to advance the floating wind technology.

All the reasoning is made with reference to a floating wind turbine in particular, but it is deemed valid for any FOWT. The floating wind turbine of reference is based on an open-source concept and is defined in Section 2. The idea is to use the tools of multivariable systems control to gain insight about the effects of waves on the FOWT response and to assess which is the best control to mitigate them. Then, to leverage this knowledge to design a feedforward controller that reduces the power fluctuations caused by waves. A control-oriented linear model of the FOWT is required first for the multivariable analysis, and later for the synthesis of the feedforward controller. The control-oriented linear model is briefly introduced in Section 3. Section 4 deals with the input-output analysis. The feedforward controller is designed in Section 5. Again, linear analysis is utilized to assess the controller performance, which is shown to be highly dependent on the wind turbine operating point. Hence, a gain-scheduling law is introduced have the maximum performance in any wind condition. The wave-feedforward controller requires as input a preview of the incoming waves, which is obtained based on the algorithm presented in Section 6. In Section 7, the feedforward controller and the wave prediction algorithm are implemented in a nonlinear, medium-fidelity model of the floating wind turbine, and numerical simulations are carried out in realistic environmental conditions to evaluate the benefits of the feedforward control strategy. Section 8 draws the conclusion and gives some recommendations for future work.

2 Definition of a reference floating wind turbine

This section defines the floating system that is considered in this study. The FOWT is formed by the DTU 10MW Bak et al. (2013) wind turbine and the INNWIND.EU TripleSpar platform Azcona et al. (2017); Lemmer et al. (2020). The characteristics of this FOWT concept are similar to those of the current commercial projects, and are publicly available.

The wind turbine is regulated with an industry-standard generator-speed controller. In below-rated winds the controller maximizes the extracted power by keeping the blade pitch angle θ constant and varying the generator torque Q_G as a function of generator speed ω_G squared:

$$Q_G = k_G \omega_G^2 \,, \tag{1}$$

https://doi.org/10.5194/wes-2021-9
Preprint. Discussion started: 1 March 2021

eawe european academy of wind energy
Open Access WIND ENERGY SCIENCE DISCUSSIONS

with $k_G = \frac{1}{2}\rho\pi R^5 \left(C_{p,max}/\tau^3\lambda_{opt}^3\right)$, where ρ is the air density, R the rotor radius, and τ the transmission ratio. $C_{p,max}$ is the maximum power coefficient, which is achieved for zero pitch angle and the optimal tip-speed-ratio λ_{opt}.

In above-rated winds, the controller regulates the extracted power to its rated value setting the generator torque to a constant value, equal to rated. Generator speed oscillations are directly reflected by the wind turbine power output. The rotor speed is regulated to its rated value $\omega_{G,r}$ by the CPC, which reacts to the generator speed feedback as:

$$\theta = k_P(\omega_G - \omega_{G,r}) + k_I \int (\omega_G - \omega_{G,r})dt\,, \tag{2}$$

where k_P and k_I are the proportional and integral gains, which are tuned following the model-based approach of Fontanella et al. (2018) to achieve the maximum damping for the platform pitch mode and for the drivetrain mode. A gain scheduling factor is introduced to adjust the PI controller gains as the wind speed varies. The generator-speed feedback controller constitutes the baseline configuration against which the benefits of feedforward are assessed.

3 The control-design model

Feedforward control is a model-based control strategy and its development requires a linear model of the floating wind turbine. The control-design model is derived based on linear first-principle equations of the most important physics of the FOWT, rather than from the linearization of a higher-order model. The main features of the model are recalled below, while a detailed description is found in Fontanella et al. (2020).

The model is built to describe the global dynamics of the FOWT and neglects the dynamics of single components. It considers the rigid-body platform motions and the rotor dynamics about a steady-state configuration (operating-point) set by an average wind speed, static displacement of the platform, rotor speed, collective-pitch and generator torque. The inputs are generator torque and collective blade-pitch angle, which are the main control variables for the FOWT, in addition to wind turbulence and wave elevation. The model equations are cast in state-space form and are valid only for small perturbations about the operating-point.

The structural dynamics builds on the theory of multibody systems. The model considers the FOWT components as rigid bodies: this simplification is deemed acceptable in a control-oriented model, as the bandwidth of an FOWT controller is usually lower than the flexible modes of the tower, blades and drivetrain. Moreover, the focus of the control-oriented model is the coupled rotor-platform response induced by waves more than the dynamics of the flexible components.

Rotor aerodynamics are introduced in the model with a simplified approach. The aerodynamic model does not consider the single blade, but computes the integral rotor forces. This simplification is valid because the global dynamics of the FOWT is determined by the integral rotor loads, rather than the loads of the single blades Lemmer (ne Sandner). Only the rotor torque and thrust force are taken into account because they drive the global dynamics of the floating turbine: aerodynamic torque sets the wind turbine power production and thrust force the motion of the floating platform. Torque and thrust are modeled by means of the quasi-steady approach, based on the derivatives of the torque and thrust curves of the wind turbine. The formulation of the control-oriented model enables the inclusion of the unsteady aerodynamic effects associated with the motion of the FOWT,

https://doi.org/10.5194/wes-2021-9
Preprint. Discussion started: 1 March 2021

eawe european academy of wind energy
Open Access WIND ENERGY SCIENCE DISCUSSIONS

which may have an influence on the dynamics of the platform modes. In this respect, a similar approach to the one presented in Bayati et al. (2017) could be used.

3.1 Frequency-dependent hydrodynamic loads

Hydrodynamic radiation and first-order-wave forces are modeled by means of linear-time-invariant parametric models.

The frequency-dependent radiation forces are approximated by a parametric model in state-space form, from the added mass and damping matrices of panel code pre-calculations. In this work, the frequency domain identification method of the MATLAB toolbox developed in Perez and Fossen (2009) is used, but other methods are available in literature Janssen et al. (2014).

Also the first-order-wave excitation is introduced in the model with a parametric model in state-space form, which connects the wave elevation to the wave forces. This choice allows to have the wave elevation, rather than wave forces, as input to the model. The wave excitation model is obtained based on the wave-force coefficients, which are usually computed at discrete frequencies through a panel code (e.g. WAMIT WAM). In the present case, the parametric model is defined by means of system identification of the impulse response function of the force coefficients Jonkman et al. (2018); Lemmer (ne Sandner), whereas frequency-domain data (i.e. the force coefficients) are used for identification in Al et al. (2020). The wave-force model of panel code data is non-causal, which means a force is developed before the wave reaches the center of the platform. The panel code data, in the form of impulse response functions, are causalized before system identification by introducing a time delay t_d (with $t_d > 0$) to have zero response for negative times. The time delay is embedded inside the identified parametric model and, consequently, into the linear model of the FOWT. The response obtained from the linear model is delayed of a time t_d with respect to the input wave elevation.

4 Input-output analysis

An input-output analysis is carried out to gain insight into the FOWT response to the available controls, generator torque and collective-pitch, and to the wave disturbance. The analysis answers the question of which is the best combinations of controls to be used to reject the detrimental effects of waves. This information is used later on to support the synthesis of the feedforward control strategy. Moreover, the analysis gives a picture of the FOWT dynamics that may prove to be useful also for other purposes.

The analysis starts from the control-design model in a transfer function representation

$$\boldsymbol{y} = \boldsymbol{G}\boldsymbol{u} + \boldsymbol{G}_d\boldsymbol{d}. \tag{3}$$

The system has two outputs, rotor speed and tower-top motion, which are collected in $\hat{\boldsymbol{y}} = [\omega_r,\ x_{tt}]^T$; two control inputs, collective-pitch and generator torque, collected in $\hat{\boldsymbol{u}} = [\theta,\ Q_g]^T$; and two disturbance inputs, the variation from average of the hub-height wind speed and the wave elevation, $\hat{\boldsymbol{d}} = [v,\ \eta]^T$. The model of Eq. (3) is used to compute the deviation of the outputs from their steady-state value, because of a change in the control and disturbance inputs.

https://doi.org/10.5194/wes-2021-9
Preprint. Discussion started: 1 March 2021

eawe european academy of wind energy
Open Access WIND ENERGY SCIENCE DISCUSSIONS

To make it easier to interpret the results of the MIMO analysis, the model of Eq. (3) needs to be scaled. This ensures that inputs and outputs are of the same importance. The scaled model is obtained by dividing any variable by its maximum expected (for the disturbances) or allowed (for the control inputs) change. The output, input and disturbance scaling matrices (D_y, D_u and D_d respectively) are

$$\boldsymbol{D}_y = \begin{bmatrix} 0.15\omega_0 & 0 \\ 0 & 5 \end{bmatrix}, \qquad \boldsymbol{D}_u = \begin{bmatrix} 5\pi/180 & 0 \\ 0 & 0.1Q_{g,0} \end{bmatrix}, \qquad \boldsymbol{D}_d = \begin{bmatrix} 0.1U & 0 \\ 0 & 4 \end{bmatrix}, \tag{4}$$

where ω_0 is the rated rotor speed, $Q_{g,0}$ the rated generator torque, and U the mean wind speed. The scaled model is

$$\hat{\boldsymbol{y}} = \hat{\boldsymbol{G}}\hat{\boldsymbol{u}} + \hat{\boldsymbol{G}}_d\hat{\boldsymbol{d}}, \tag{5}$$

with

$$\hat{\boldsymbol{G}} = \boldsymbol{D}_y^{-1}\boldsymbol{G}\boldsymbol{D}_u\,, \qquad \hat{\boldsymbol{G}}_d = \boldsymbol{D}_y^{-1}\boldsymbol{G}_d\boldsymbol{D}_d\,. \tag{6}$$

Given an input between 0 and 1, where 0 is no input and 1 is the maximum expected value, the outputs of the model of Eq. (5) take a value between 0 and 1, where 0 is no output and 1 corresponds to the maximum expected or allowed value for the output.

4.1 Control inputs

The model without disturbances $\hat{\boldsymbol{y}} = \hat{\boldsymbol{G}}\hat{\boldsymbol{u}}$ is considered first. The transfer function matrix $\hat{\boldsymbol{G}}$ has two couples of input and output directions, each with an associated gain. For any selected frequency, the directions and gains of matrix $\hat{\boldsymbol{G}}$ are obtained from its singular value decomposition (SVD) Levine (1996)

$$\hat{\boldsymbol{G}} = \boldsymbol{U}\boldsymbol{\Sigma}\boldsymbol{V}^H\,. \tag{7}$$

The column vectors of $\boldsymbol{V} = [\overline{\boldsymbol{v}},\ \underline{\boldsymbol{v}}]$ are the input directions, the column vectors of $\boldsymbol{U} = [\overline{\boldsymbol{u}},\ \underline{\boldsymbol{u}}]$ the output directions, and the respective singular values are along the diagonal of $\boldsymbol{\Sigma} = \mathrm{diag}(\overline{\sigma},\ \underline{\sigma})$. When the input vector $\hat{\boldsymbol{u}}$ has the same direction of vector $\overline{\boldsymbol{v}}$, the output $\hat{\boldsymbol{y}}$ is along the direction $\overline{\boldsymbol{u}}$, the gain is equal to $\overline{\sigma}$ and it is the largest possible for that frequency. The input produces the most effect on the output, and the directions of $\overline{\boldsymbol{v}}$ and $\overline{\boldsymbol{u}}$ are named the *strongest*. Conversely, when the input is directed as $\underline{\boldsymbol{v}}$, the gain is $\underline{\sigma}$, and the input has the least effect on the output, which is along $\underline{\boldsymbol{u}}$. The directions of $\underline{\boldsymbol{v}}$ and $\underline{\boldsymbol{u}}$ are named the *weakest*.

The steady-state (i.e. zero frequency) plant model of the FOWT in a 16 m/s wind is

$$\hat{\boldsymbol{G}}(j\omega = 0) = \begin{bmatrix} -2.736 & -0.311 \\ -1.216 & 0.097 \end{bmatrix}. \tag{8}$$

The (1,1) element of $\hat{\boldsymbol{G}}$ is much larger than the (1,2) element, so the rotor speed is a lot more sensitive to a steady-state (i.e. a very slow) change in collective-pitch, the first input, than in generator torque, the second input. Collective-pitch effects both

https://doi.org/10.5194/wes-2021-9
Preprint. Discussion started: 1 March 2021

eawe european academy of wind energy
Open Access WIND ENERGY SCIENCE DISCUSSIONS

rotor speed, the first output, and tower-top motion, the second output, in the same direction. If collective-pitch is increased, the rotor is slowed because of the decreased aerodynamic torque, and the nacelle moves upwind, because of the lower thrust force. The plant model is decomposed into its SVD

$$\boldsymbol{U} = \begin{bmatrix} -0.916 & -0.401 \\ -0.401 & 0.916 \end{bmatrix}, \qquad \boldsymbol{\Sigma} = \begin{bmatrix} 3.004 & 0 \\ 0 & 0.214 \end{bmatrix}, \qquad \boldsymbol{V} = \begin{bmatrix} 0.997 & -0.082 \\ 0.082 & 0.997 \end{bmatrix}. \tag{9}$$

The strongest and weakest input directions are obtained by different combinations of collective-pitch and generator torque (e.g. the strongest is given by 0.997 of collective-pitch and 0.082 of generator torque). The ratio between the gain in the strongest and weakest direction (i.e. the condition number) is $\mathrm{CN} = \overline{\sigma}/\underline{\sigma} = 14.0$. The system is said to be *ill-conditioned*. At steady-state, the input combinations with prevailing collective-pitch have a much stronger effect on the FOWT than the input combinations with prevailing generator torque. The strongest and weakest output directions are given by different combinations of rotor speed and tower-top motion. From $\overline{\boldsymbol{u}} = [-0.916,\ -0.401]^T$, it is seen that the effect of the strongest input combination, an increase of collective-pitch, is to slow down the rotor and to move the nacelle upwind. This is in agreement with the result of the inspection of $\hat{\boldsymbol{G}}(j\omega = 0)$ and makes sense from a physical point of view.

The SVD of the plant model $\hat{\boldsymbol{G}}(j\omega)$ is computed for several frequencies up to 0.3 Hz, and for seven operating points for wind speeds between 12 and 24 m/s. The top plot of Fig. 1 shows the magnitude of the two component of $\overline{\boldsymbol{u}}$, that is the fraction of collective-pitch and generator torque in the strongest input combination; the middle plot, the magnitude of the first and second component of $\overline{\boldsymbol{v}}$, the fraction of rotor speed and tower-top motion in the strongest output direction; the bottom plot the corresponding singular values, the gain. Collective-pitch is the most effective input, at any frequency and in any above-rated wind speed. Collective-pitch effects both rotor speed and tower top motion, because it modifies at the same time the aerodynamic torque and thrust. At the platform modes frequencies, the response is almost only tower-top motion and the gain is increased. It takes a small collective-pitch action to move the nacelle, because the resulting rotor thrust variation excites the resonant response of the platform. Controlling rotor speed is hard. In the wave frequency range, the gain is decreased so it becomes more difficult to control the system, and rotor speed is easier to control than tower-top motion.

In summary, collective-pitch is the most effective control in above-rated winds. It effects both rotor speed and tower-top motion. In the frequency range where wave is active, collective-pitch becomes less effective, so it is harder to control the wind turbine.

4.2 Disturbances

The wind and waves disturbances are here considered separately. The direction of a disturbance is

$$\boldsymbol{y}_d = \frac{1}{\|\hat{\boldsymbol{g}}_d\|_2} \hat{\boldsymbol{G}}_d\,, \tag{10}$$

where $\hat{\boldsymbol{g}}_d$ is the appropriate column of $\hat{\boldsymbol{G}}_d$ (the first for wind, the second for wave). The disturbance condition number is

$$\mathrm{DCN} = \overline{\sigma}(\hat{\boldsymbol{G}})\overline{\sigma}(\hat{\boldsymbol{G}}^{-1}\boldsymbol{y}_d)\,, \tag{11}$$

https://doi.org/10.5194/wes-2021-9
Preprint. Discussion started: 1 March 2021

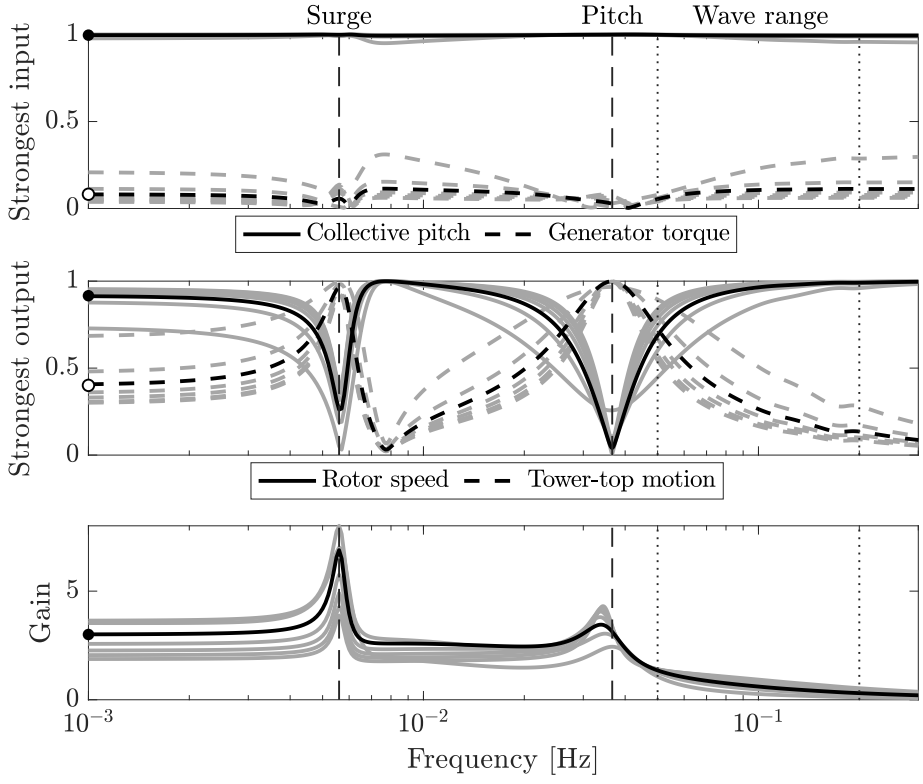

Figure 1. Singular value decomposition of the floating wind turbine plant for several above-rated operating points (grey), and for the 16 m/s wind case (black) with values for the zero-frequency case displayed by the marks • and ○. The vertical dashed lines are the frequency of the platform surge and pitch modes, the frequency range where waves are active is enclosed by the vertical dotted lines.

where $\overline{\sigma}(\cdot)$ is the maximum singular value. The DCN measures the control effort required to reject a given disturbance, relative to rejecting a disturbance with the same magnitude but aligned with the strongest output direction (i.e. the direction where controls are effective the most) Skogestad and Postlethwaite (2005). The higher the DCN is, the harder it is to reject the disturbance with the available controls.

The effects of the wind and waves disturbance in the frequency range up to 0.3 Hz is assessed in Fig. 2, for seven operating points of wind speed between 12 and 24 m/s. Wind turbulence acts directly on the rotor causing, first, a variation of the aerodynamic torque, which affects rotor speed. Wind turbulence also acts on the platform, through the rotor thrust, but this excitation mechanism is less effective than wave forcing. The wind disturbance is aligned to the rotor speed output direction. Collective-pitch is very effective for controlling rotor speed, and rejecting the wave disturbance with collective-pitch does not require a large effort. This is visualized by the DCN. Wave is aligned to tower-top motion, and partially shifts towards rotor speed for increasing frequency. Waves act on the platform, but also excite rotor speed. The platform motion caused by waves, turns out into a variation of the apparent wind speed, which affects rotor torque, and then speed. This mechanism of excitation

https://doi.org/10.5194/wes-2021-9
Preprint. Discussion started: 1 March 2021

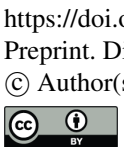

eawe european academy of wind energy
Open Access WIND ENERGY SCIENCE DISCUSSIONS

is more effective above the platform pitch frequency, because most of the wave energy is concentrated here. The gain of waves is maximum at the platform modes frequencies, where wave excites the FOWT in resonance causing large motions, and in the wave range. The wave disturbance is not aligned to the rotor speed output direction, and the DCN shows that it is very hard to counteract the wave disturbance by means of the wind turbine controls.

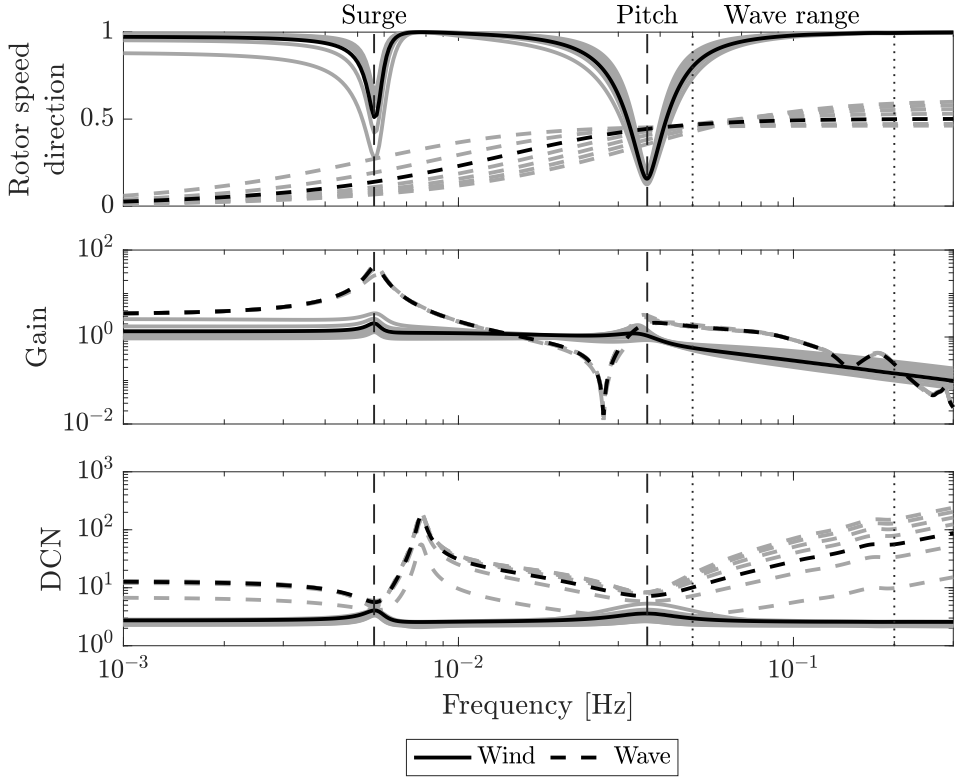

Figure 2. The direction with respect to the rotor speed output direction, the singular value (gain) and the disturbance condition number (DCN) associated to wind and waves. Grey lines correspond to the above-rated operating points and the black line to the 16 m/s wind speed case. The vertical dashed lines are the frequency of the platform surge and pitch modes, the frequency range where waves are active is enclosed by the vertical dotted lines.

To sum up, waves effect rotor speed, because waves drive the platform motion which result into an apparent wind speed at rotor. The wave excitation is stronger at the platform frequencies, where the FOWT is excited in resonance, and in the wave range, where it is concentrated most of the wave energy. Moreover, it is quite hard to counteract the wave disturbance by means of the wind turbine controls. All this shows that new control strategies specific to FOWTs are needed to deal with waves. The wave-feedforward control strategy leverages the knowledge of the FOWT dynamics to improve the performance of the traditional wind turbine controller with respect to the mitigation of the wave effects.

https://doi.org/10.5194/wes-2021-9
Preprint. Discussion started: 1 March 2021

eawe european academy of wind energy
Open Access WIND ENERGY SCIENCE DISCUSSIONS

5 The wave-feedforward control strategy

The feedforward (FF) controller is designed to cancel the effect of the wave disturbance on rotor speed, end hence on the power output of the wind turbine. The FF controller regulates rotor speed producing an additional collective-pitch request which is summed to the pitch signal of the existing generator-speed feedback (FB) controller. The FBFF control strategy is shown in 3.

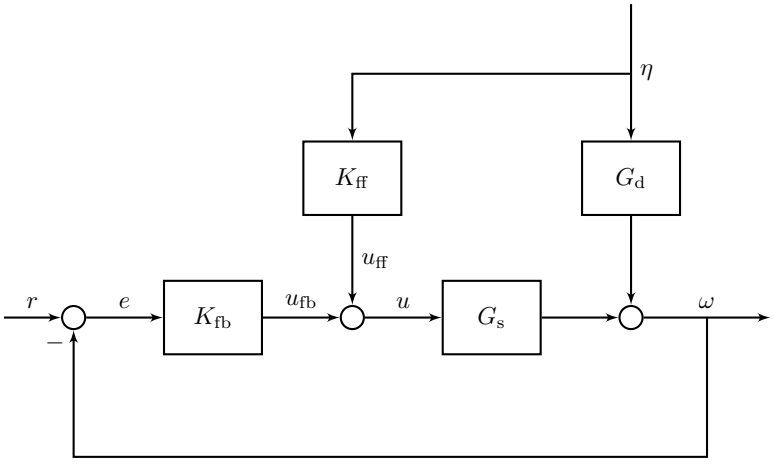

Figure 3. Block diagram of the feedback-feedforward controller.

For wave-disturbance rejection, the reference signal r is zero and the closed-loop rotor speed output ω is

$$\omega = (I + G_s K_{\mathrm{fb}})^{-1}(G_s K_{\mathrm{ff}} + G_d)\eta \,, \tag{12}$$

where, G_s is the collective-pitch to rotor-speed plant, G_d the wave disturbance model, K_{fb} the FB controller, K_{ff} the FF controller, η the wave disturbance. In the model-inverse approach, the FF controller K_{ff} is designed to cancel the effect of η on ω, thus the transfer function of the controller is

$$K_{\mathrm{ff}} = -G_s^{-1} G_d \,. \tag{13}$$

K_{ff} is the transfer function between the input wave elevation measurement and the collective-pitch command. In general, G_s, G_d, and K_{ff}, depend on the wind turbine operating condition and so, on the mean wind speed.

The transfer function of the FF controller obtained based on Eq. (13), which was evaluated for different wind conditions, is shown in Fig. 4. There is a significant difference between the generic shape assumed by K_{ff} in below-rated and above-rated conditions. The amplitude is increased in below-rated winds because collective-pitch is not effective for controlling rotor speed. There, a variation of the collective-pitch produces a smaller variation of rotor torque than in above-rated winds. For this reason, it is decided to confine the action of the FF controller to the above-rated region: when the mean pitch angle falls below a threshold, the FF action is switched off in order to prevent an excessive pitch actuators usage.

https://doi.org/10.5194/wes-2021-9
Preprint. Discussion started: 1 March 2021

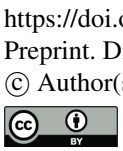

eawe european academy of wind energy
Open Access WIND ENERGY SCIENCE DISCUSSIONS

The above-rated controller K_{ff} has a peak at the platform pitch natural frequency which is not present in below-rated winds. In above-rated winds, the platform pitch mode damping is decreased and the wave excitation leads to a large response at this frequency. This causes significant oscillations of the tower-top, with consequently large variations of the apparent wind speed. A high control effort is therefore required to balance the wind fluctuations.

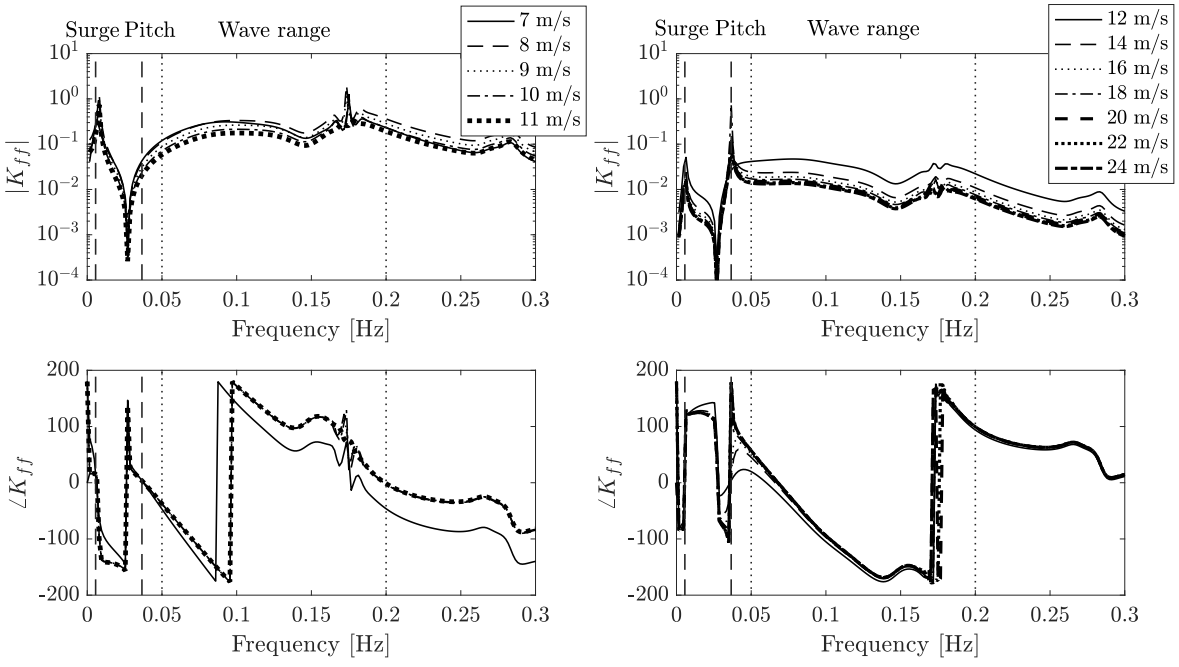

Figure 4. The feedforward controller transfer function K_{ff} for below-rated (left) and above-rated (right) operating conditions. The vertical dashed lines are the frequency of the platform surge and pitch modes, the frequency range where waves are active is enclosed by the vertical dotted lines.

220

5.1 Disturbance rejection analysis

Considering the FBFF controller of Fig. 3, and the closed-loop disturbance response of Eq. (12), the FB, the FF and the FBFF sensitivity function is defined respectively as

$$S_{\mathrm{fb}} = (1 + G_s K_{\mathrm{fb}})^{-1} ,$$
$$S_{\mathrm{ff}} = 1 + G_s K_{\mathrm{ff}} G_d^{-1} ,$$
$$S_{\mathrm{fbff}} = S_{\mathrm{fb}} S_{\mathrm{ff}} . \tag{14}$$

https://doi.org/10.5194/wes-2021-9
Preprint. Discussion started: 1 March 2021

eawe european academy of wind energy
Open Access WIND ENERGY SCIENCE DISCUSSIONS

The sensitivity function of the FBFF controller is computed for different above-rated wind speeds U_i to account for the different behavior of the wind turbine

$$
\begin{aligned}
S_{\mathrm{fbff}}(U_i) &= S_{\mathrm{fb}}(U_i) S_{\mathrm{ff}}(U_i) \ , \\
S_{\mathrm{fb}}(U_i) &= (1 + G_s(U_i) K_{\mathrm{fb}}(U_i))^{-1} \ , \\
S_{\mathrm{ff}}(U_i) &= 1 + G_s(U_i) K_{\mathrm{ff}}(\overline{U}) G_d^{-1}(U_i) \ ,
\end{aligned} \tag{15}
$$

with $U_i = 12, 13, \ldots, 24\ m/s$ and $\overline{U} = 16\ m/s$.

The disturbance-rejection function is derived from the sensitivity function and it directly relates the wave disturbance to the closed-loop rotor speed. For the FB and the FBFF controllers it is defined respectively as

$$
\begin{aligned}
T_{\mathrm{fb}} &= S_{\mathrm{fb}} G_d \ , \\
T_{\mathrm{fbff}} &= S_{\mathrm{fbff}} G_d \ .
\end{aligned} \tag{16}
$$

The disturbance-rejection function of the FB and FBFF controllers at 16 m/s wind speed is shown in Fig. 5 (thick solid line and thin dotted line). The magnitude of T_{fb} is increased in correspondence of the platform pitch mode and at higher frequencies. Collective-pitch FB control results into a decreased damping of the (closed-loop) pitch mode Larsen and Hanson (2007); van der Veen et al. (2012) and consequently, to a large resonant response, which translates into large fluctuations of the apparent wind speed at the platform pitch frequency. The bandwidth of the FB controller is 0.0186 Hz. This low value is the consequence of the gain detuning required to stabilize the FOWT van der Veen et al. (2012); Lackner (2009); Fontanella et al. (2018); Lemmer (ne Sandner). Above this frequency the controller does not react to the wind speed fluctuations associated to the wave disturbance. T_{fbff} is higher than T_{fb} around the platform pitch natural frequency. Combining the FB controller with the FF controller strengthens the coupling between platform pitch and rotor speed.

The disturbance-rejection function of the FBFF controller is computed for different above-rated wind speeds U_i

$$
T_{\mathrm{fbff}}(U_i) = S_{\mathrm{fbff}}(U_i) G_d(U_i) \ . \tag{17}
$$

with $U_i = 12, 13, \ldots, 24\ m/s$ and $S_{\mathrm{fbff}}(U_i)$ already obtained in Eq. (15). The magnitude of $T_{\mathrm{fbff}}(U_i)$ is shown in Fig. 5. The disturbance-rejection function, and so the performance of the FBFF controller, is sensitive to the mean wind speed. This is due to the rotor aerodynamics which changes for different operating conditions. The benefit of the additional FF controller is maximum at 16 m/s, the operating point considered for model inversion, lower elsewhere, and minimum in 12 m/s wind.

5.2 Gain scheduling

The wave disturbance effect on the FOWT is sensitive to the mean wind speed. To have the maximum possible reduction of the wave disturbance, the FF controller needs to take into account how the FOWT dynamics are modified with the operating condition.

Based on the procedure introduced above, a linear model of the FOWT is computed for several above-rated wind speeds and, by means of Eq. (13), an FF controller is obtained for each of them. The transfer function of the FF controllers is shown

https://doi.org/10.5194/wes-2021-9
Preprint. Discussion started: 1 March 2021

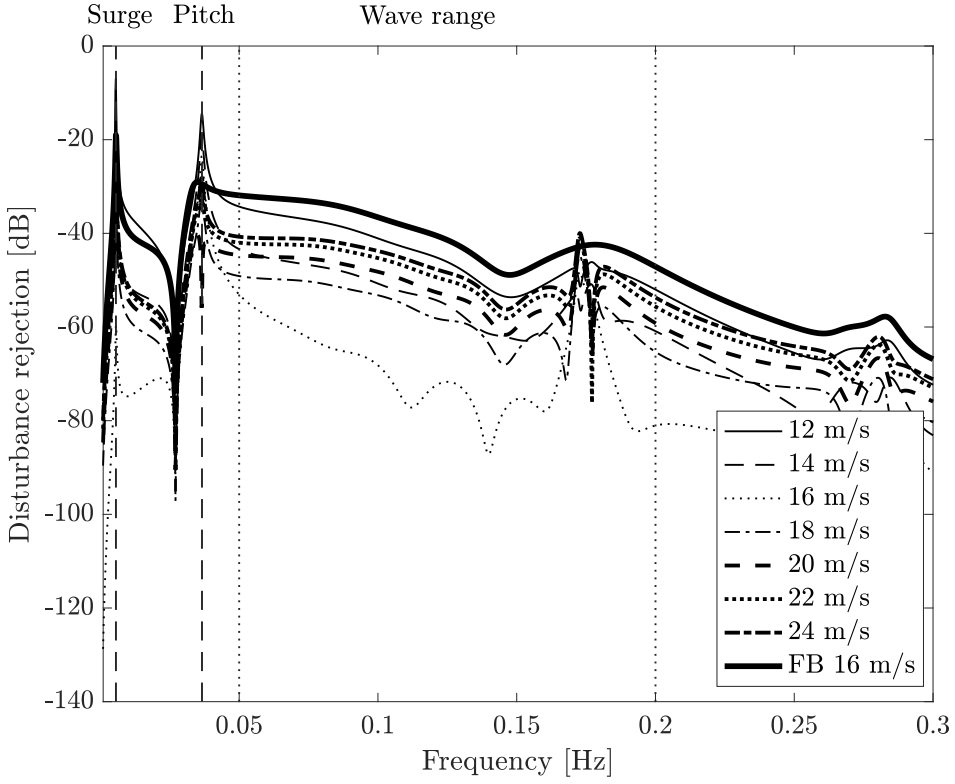

Figure 5. Disturbance-rejection function of the feedback-feedforward controller in above-rated winds. The feedback controller (FB) in 16 m/s wind is reported for comparison. The vertical dashed lines are the frequency of the platform surge and pitch modes, whereas the frequency range where waves are active is enclosed by the vertical dotted lines.

in Fig. 6. From visual inspection of the figure, it is evident that the effort required to cancel the wave disturbance is maximum in near-rated winds and decreases in high winds. If the FF controller obtained from the 16 m/s model is used at any wind speed, the FF action would be less-than-ideal for wind speeds between rated and 16 m/s, and higher-than-ideal for greater wind speeds, leading to a decreased performance as highlighted by the disturbance rejection analysis of Fig. 5.

Figure 6 also reveals the shape of the FF controller does not change much with wind speed except for the static gain. Based on this consideration, the performance of the FF controller is improved by adjusting the static gain based on the actual wind turbine operating condition. In other words, a single FF controller is computed for the 16 m/s condition and the static gain is modified as the wind speed changes, to reflect the different dynamics of the FOWT. The actual collective-pitch angle is chosen as the scheduling variable. The gain-scheduling law is obtained fitting a quadratic function to the DC-gain of the $K_{\mathrm{ff}}(j\omega)$ computed for different above-rated winds. The scheduled FF controller is

$$K_{\mathrm{ff}}(\beta) = c_{\mathrm{ff}}(\beta) K_{\mathrm{ff}}(\overline{U}) \,,$$
$$c_{\mathrm{ff}}(\beta) = p_2\beta^2 + p_1\beta + p_0 \,, \tag{18}$$

https://doi.org/10.5194/wes-2021-9
Preprint. Discussion started: 1 March 2021

eawe european academy of wind energy
Open Access WIND ENERGY SCIENCE DISCUSSIONS

where p_2, p_1, p_0 are the coefficients of the quadratic best-fit function, β is collective-pitch, and $K_{\text{ff}}(\overline{U})$ is the FF controller for 16 m/s wind speed.

In Fig. 6, the scheduled FF controllers $K_{\text{ff}}(\beta) = c_{\text{ff}}(\beta)K_{\text{ff}}(\overline{U})$ are compared to the model-inversion FF controllers obtained from the evaluation of Eq. (13) for different above-rated wind speeds. The scheduled controller is a good approximation of the ideal case. The proposed scheduling strategy leaves the phase of $K_{\text{ff}}(j\omega)$ unchanged, but this is acceptable since the phase does not change much with wind speed.

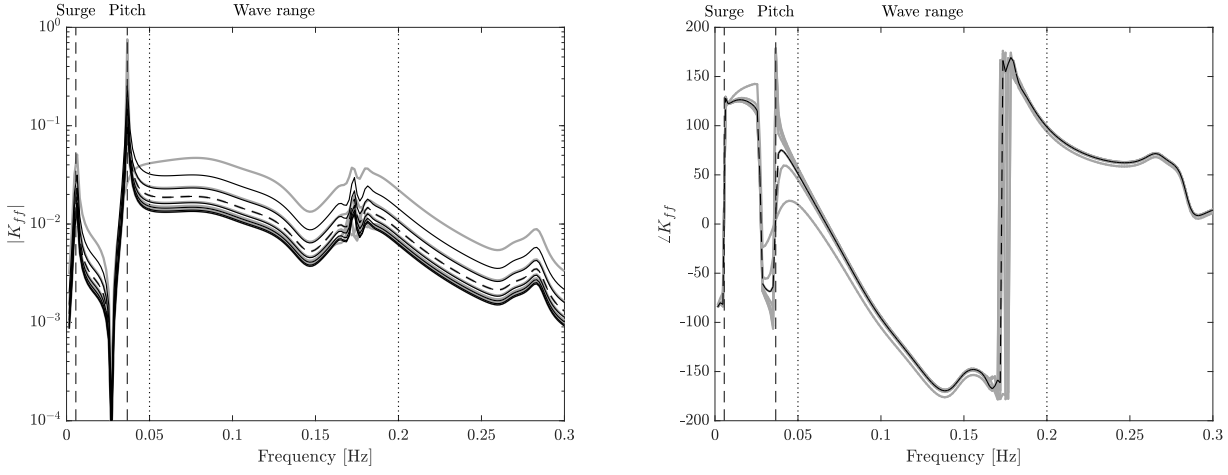

Figure 6. The scheduled feedforward controllers $K_{\text{ff}}(\beta) = c_{\text{ff}}(\beta)K_{\text{ff}}(\overline{U})$ (black) obtained from the scheduling of the 16 m/s controller $K_{\text{ff}}(\overline{U})$ (dashed) are compared to the model inversion controllers $K_{\text{ff}}(U_i)$ (grey) for different above-rated wind speeds $U_i = 12, 13, \ldots, 24\ m/s$. Magnitude (left) and phase (right). Wave range is the frequency range where linear wave is active.

The disturbance rejection function of the FBFF controller with scheduling is obtained by replacing $K_{\text{ff}}(\overline{U})$ with $K_{\text{ff}}(\beta)$ in Eq. (15) and Eq. (17) and it is shown in Fig. 7. The disturbance rejection in the wave frequency range is lower for any wind speed, as the controller action is adjusted based on the wind turbine operating condition.

The FF controller for implementation is obtained as in Eq. (18). The order of the transfer function $K_{\text{ff}}(\overline{U})$ is too high for practical usage: a reduced-order approximation is utilized in place of the original transfer function. The low-pass filtered collective-pitch angle measurement is used for scheduling.

6 Wave measurement and prediction

The transfer function of the FF controller has an intrinsic delay of t_d. A suitable wave elevation measurement is required to compensate the intrinsic delay of the FF controller: it is required to know the wave t_d before it arrives at the platform. The wave prediction is obtained from a measurement of the surface elevation in a point at a distance l upstream the platform. The measurement is propagated downstream in space and forward in time.

https://doi.org/10.5194/wes-2021-9
Preprint. Discussion started: 1 March 2021

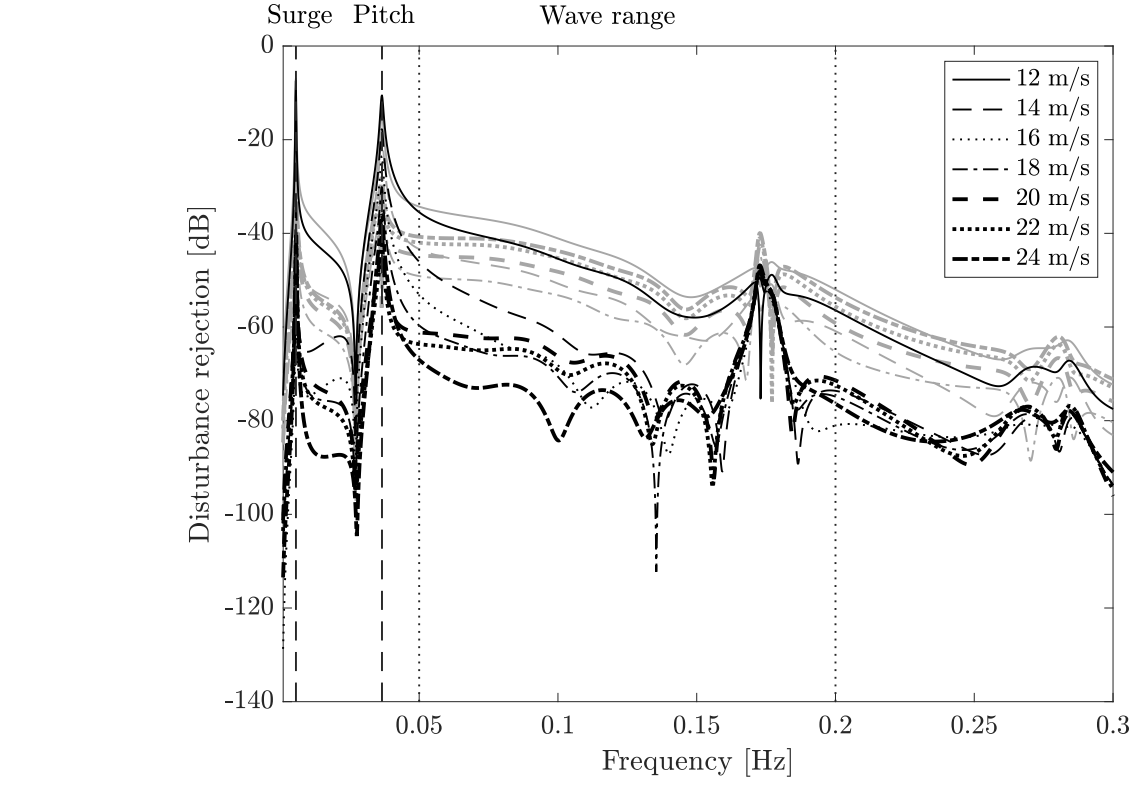

Figure 7. Disturbance rejection of the FBFF controller with scheduling (black) and without (grey), for several above-rated operating conditions. The vertical dashed lines are the frequency of the platform surge and pitch modes, the frequency range where waves are active is enclosed by the vertical dotted lines.

The wave elevation in two points along the wave propagation direction is related by the frequency response function

$$H_l = e^{-jkl}, \tag{19}$$

where k is the wave number, and, for gravity waves on deep-water, $k \approx \omega^2/g$.
The frequency response function that relates the upstream wave measurement to the wave prediction at the FOWT is

$$H(j\omega) = e^{j\omega\left(t_d - \frac{\omega l}{g}\right)}. \tag{20}$$

For a given distance l and a preview time of t_d, $H(j\omega)$ behaves as a pure negative-delay operator only for $\omega > gt_d/l = \omega_t$. The wave spectral components with a frequency greater than ω_t are successfully predicted. Prediction of the wave components with a lower frequency is not possible, because the wave arrives at the platform location in a time lower than the preview time t_d. It is possible to predict the lower-frequency harmonics by measuring the wave elevation far upstream the FOWT or by decreasing the preview time.

https://doi.org/10.5194/wes-2021-9
Preprint. Discussion started: 1 March 2021

eawe european academy of wind energy
Open Access WIND ENERGY SCIENCE DISCUSSIONS

For real-time control purposes, the wave prediction model of Eq. (20) is implemented as it is shown in Fig. 8. The wave elevation η is continuously measured in l meters upstream the floating wind turbine with a sample rate T_s. At any time instant t_k, the discrete Fourier transform (DFT) of the last n samples is computed to obtain the complex spectrum y. The element-wise product between y and the transfer function H, evaluated at n discrete frequencies $\omega_i = \left(2\pi i/nT_s\right),\ i = 0,\ldots,n-1$, gives the spectrum of the predicted wave elevation at platform location $\hat{y}$. The Inverse DFT of $\hat{y}$ gives $\hat{\eta}$, which is the wave elevation that is going to be experienced by floating wind turbine $d = t_d/T_s$ time samples ahead in time.

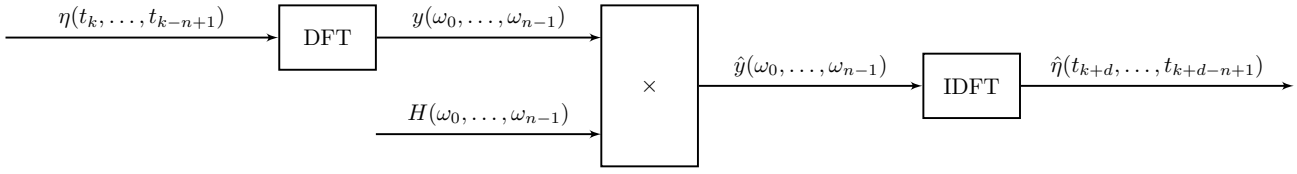

Figure 8. Scheme of the wave prediction algorithm. η is the wave elevation measurement upstream the floating wind turbine and $\hat{\eta}$ is the wave elevation at platform location, $d = t_d/T_s$ time samples ahead in time.

Several technologies are available to measure the surface elevation. Some examples are wave-rider buoy, radar, airborne or satellite. The radar technology is particularly attractive because it scans a large area, it detects waves far from its location (up to 4 km) and it is capable of fully autonomous operation. The X-band radar, commonly used by ships for navigation, received a lot of attention as a remote wave sensor. Images of the wave field are obtained from the radar as radar beams are reflected and shadowed by the crests of the wave fronts. An example of this technology is the wave monitoring system WaMoS II presented in Ziemer and Dittmer (1994) and at the base of the real-time wave-prediction system developed within the On board Wave and Motion Estimator (OWME) Reichert et al. (2010). In Naaijen and Wijaya (2014) a methodology based on 2D-FFT is proposed to obtain a directional phase-resolved prediction of the wave elevation from radar data (additional information about the directional energy spectrum is required, e.g. from a wave buoy). A similar measurement could be used in wave-FF control.

7 Results

The wave-FF control strategy is evaluated by means of numerical simulations in the servo-aero-hydro-elastic code FAST Jonkman and Marshall (2005). The FAST model has 7 DOFs: platform motions (surge, sway, heave, roll, pitch and yaw) and the rotor rotation. The drivetrain is rigid as well as the tower and blades. The hydrodynamic model is based on linear potential flow theory with viscous effects. The radiation and the first-order wave forces are computed prior to the simulation based on the same WAMIT data that are used to build the control-design model. The calculation of the frequency-dependent radiation loads is based on the convolution integral of the retardation functions matrix. Second-order wave loads are modeled by means of Newman's approximation Newman (1974).

https://doi.org/10.5194/wes-2021-9
Preprint. Discussion started: 1 March 2021

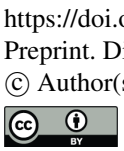

eawe european academy of wind energy
Open Access WIND ENERGY SCIENCE DISCUSSIONS

The wave-FF control strategy considered for the verification is displayed in Fig. 9. Three cases are considered: a baseline case with only FB control, the FBFF control without gain scheduling, and the FBFF control with gain scheduling. In the simulations, an ideal upstream wave measurement is used and the accuracy of the wave measurement system (e.g. radar) is not taken into account. Results are therefore indicative of the upper performance limit of wave-FF control.

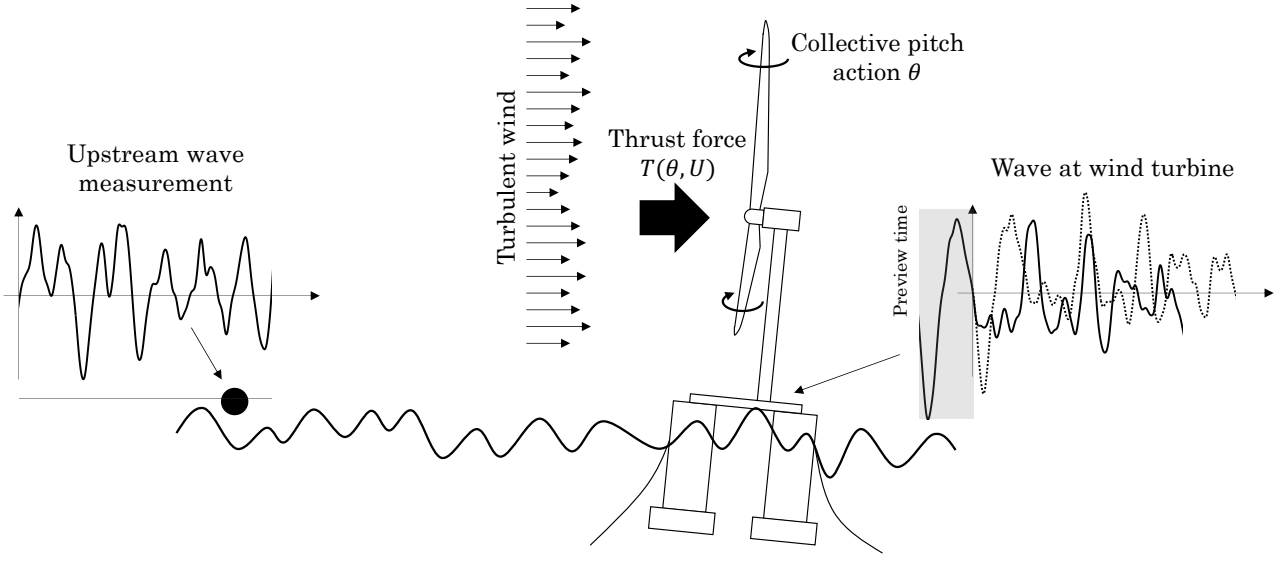

Figure 9. Schematics of the wave-feedforward control strategy. Wave excite the floating platform and generate a varying apparent wind speed for the rotor. The oscillating wind results into rotor speed fluctuations which are only partially rejected by the standard feedback controller. The feedforward action is based on the wave elevation measured upstream the wind turbine. This measurement is used to obtain a preview of the wave elevation at the floating platform, which is the input of the controller. The resulting collective-pitch action, which is summed to the pitch request from the feedback controller, counteracts the wave disturbance, modifying the aerodynamic torque and the rotor thrust force.

7.1 The environmental conditions

The floating wind turbine is subjected to three realistic turbulent wind and irregular wave combinations (see table 1), representative of an offshore site with moderate-severity met-ocean conditions. The reference site is part of the Gulf of Maine (North Atlantic ocean), about 25 km southwest of Monhegan Island and 65 km east of Portland, and the mean water depth is 130 m. Three above-rated winds were selected and, for any of them, the wave was defined from the Pierson-Moskowitz spectrum. The significant-heigh H_s and peak-period T_p were selected as the most probable combination of values for any assigned wind speed. For wind, a power-law profile with exponent 0.14 is assumed, turbulence is modeled according to the Kaimal spectrum and turbulence intensity is selected for each wind speed based on the IEC-61400, considering a wind turbine of class IC. Wind and waves are aligned to the zero-degree direction.

https://doi.org/10.5194/wes-2021-9
Preprint. Discussion started: 1 March 2021

Table 1. Metocean conditions considered for the verification of the wave-FF control strategy.

Hub-height mean wind speed [m/s]	Turbulence intensity [%]	Significant wave height [m]	Wave peak period [s]
16	12	1.5	10.0
18	11	2.5	10.0
22	10	3.5	8.0

The FB and the two FF control strategies are simulated for all the metocean conditions of table 1. For any load case, six simulations are carried out with wind and waves generated from different random seeds. Each simulation lasts 1600 s, and only the last 600 s worth of data are considered for the analysis.

7.2 Wave prediction

The wave prediction algorithm presented in section 6 is tested in the met-ocean conditions corresponding to the 16 m/s mean wind speed case of table 1. The wave elevation is sampled every 0.1 s at distance of 200 m upstream the FOWT. The wave elevation at platform location is computed based on the last 1000 samples and a preview time of 7.5 s is requested. The wave elevation preview is compared to the wave at platform in Fig. 10. The overall quality of the estimate is good. The PSD of the two signals reveals that the largest error is introduced in the low-frequency harmonics. The error is due to the intrinsic characteristics of the transfer function on which the wave prediction algorithm is based. For the present case, the transfer functions correctly predicts the wave harmonics above a threshold frequency of 0.058 Hz.

7.3 Steady wind

The effect of the FF control strategy is first demonstrated considering a steady wind without shear. With this assumption, the wave is the only disturbance acting on the FOWT. Sample time series of the rotor speed and blade pitch command for a 22 m/s wind speed case are shown in Fig. 11. The amplitude of rotor speed oscillations caused by the wave disturbance is reduced with FBFF control with respect to the FB case, and this is achieved at the expense of an increased pitch activity. The pitch effort required by the scheduled FBFF is less than without scheduling for a comparable disturbance rejection performance.

7.4 Turbulent wind

The FBFF control is evaluated in more realistic power production conditions.

Sample time series of rotor speed and blade pitch angle for the 22 m/s case are shown in Fig. 12. As visible looking at the FB case, the largest fraction of rotor speed oscillations is set by wind turbulence. This is in agreement with the MIMO disturbance

https://doi.org/10.5194/wes-2021-9
Preprint. Discussion started: 1 March 2021

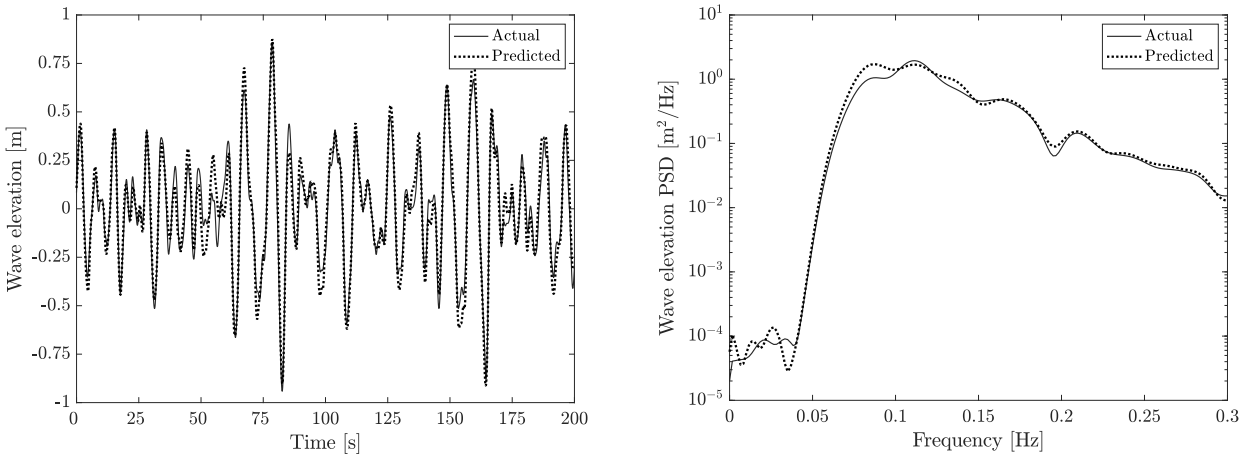

Figure 10. Left: the wave preview obtained by means of the prediction algorithm is compared with the wave at platform location (in the plot, the preview is delayed of the preview time $t_d = 7.5s$ to ease the comparison). Right: the wave preview and measurement are compared based on their PSD.

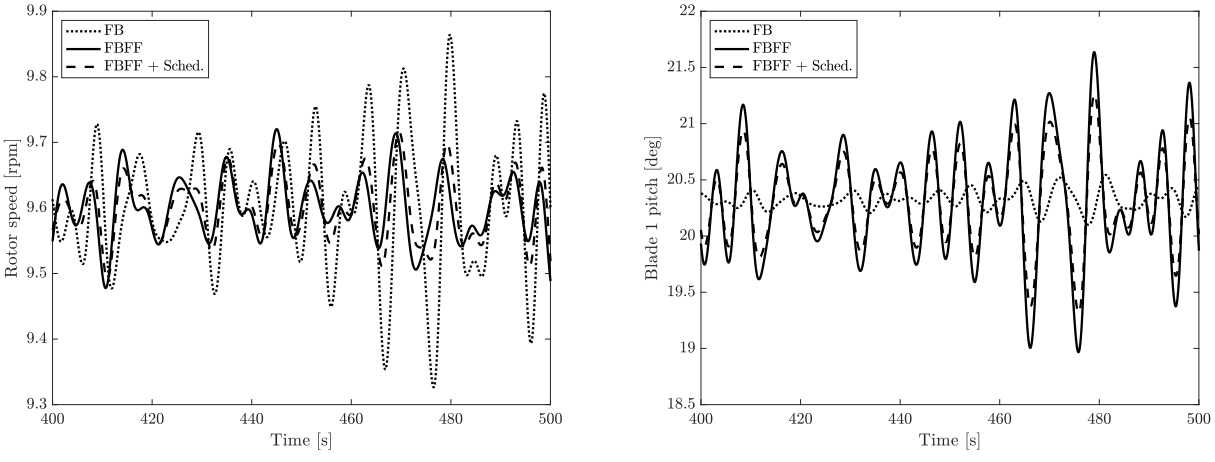

Figure 11. Time series of the rotor speed (left) and blade 1 pitch angle command (right) for the 22 m/s steady wind case.

analysis of section 4. The FF control reduces the part of rotor speed oscillations caused by waves, but it does not compensate for the effect of wind turbulence. The pitch actuation is increased with any FBFF compared to the FB case.

The power spectral density (PSD) of the rotor speed and pitch-angle-command time series of Fig. 12 is shown in Fig. 13. The FBFF achieves a clear reduction of the rotor speed dynamics in the frequency range where wave is active (0.05 Hz - 0.2 Hz), but it has a small impact at lower frequency, where the rotor speed oscillations are largely set by wind turbulence. Scheduling slightly improves the disturbance rejection and significantly lowers the control effort.

https://doi.org/10.5194/wes-2021-9
Preprint. Discussion started: 1 March 2021

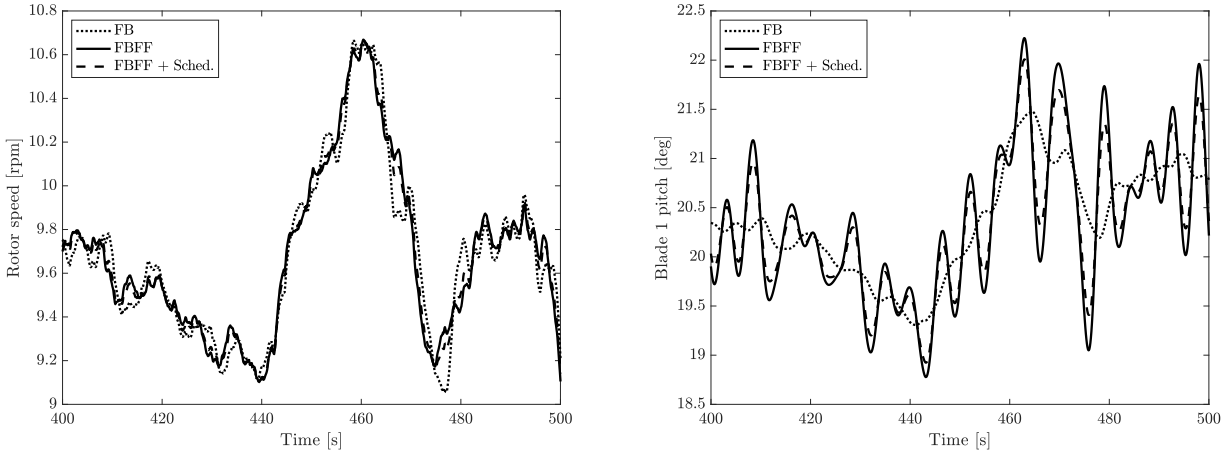

Figure 12. Time series of the rotor speed (left) and blade 1 pitch-angle-command (right) for the 22 m/s turbulent wind case.

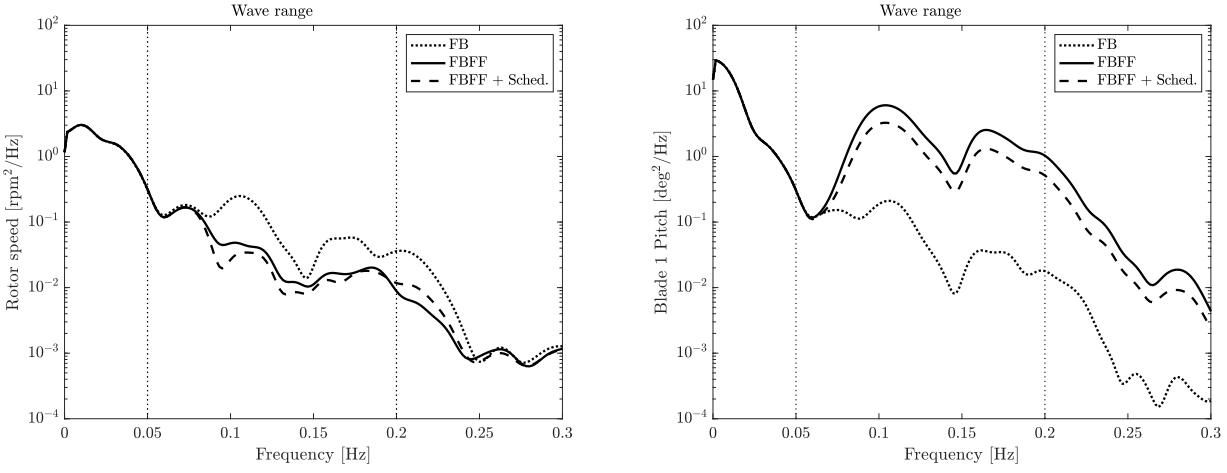

Figure 13. Power spectral density of the rotor speed (left) and blade 1 pitch angle command (right) for the 22 m/s turbulent wind case. Wave range is the frequency range where linear wave is active.

The FF control is designed to reduce the wave disturbance effect on rotor speed. However, it is expected it affects also the structural loads for the different wind turbine components and the motion of floating platform. The fatigue loads are studied in terms of damage-equivalent loads (DEL), which are calculated by means of Rainflow counting with an equivalent load frequency of 1 Hz and a Whöler exponent of 10 for the steal components (shaft, tower and mooring line) and 3 for the blades. The DEL percentage variation that is achieved with FBFF compared to FB is computed as

$$\Delta\mathrm{DEL} = \left(1 - \frac{\mathrm{DEL}_{\mathrm{FB}}}{\mathrm{DEL}_{\mathrm{FBFF}}}\right) \cdot 100\,, \tag{21}$$

https://doi.org/10.5194/wes-2021-9
Preprint. Discussion started: 1 March 2021

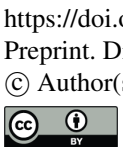

eawe european academy of wind energy
Open Access WIND ENERGY SCIENCE DISCUSSIONS

where $\mathrm{DEL}_{\mathrm{FB}}$ and $\mathrm{DEL}_{\mathrm{FBFF}}$ are the 1 Hz damage equivalent loads for the FB and the FBFF.

The DEL the FOWT components and the standard deviation of platform motions, rotor speed and blade pitch is examined in Fig. 14 for the three load cases. Only the case of FBFF with scheduling is considered. Reducing rotor speed oscillations also results into a lower fatigue damage for the wind turbine shaft and tower; platform motions are slightly increased and this is reflected into the mooring line loading.

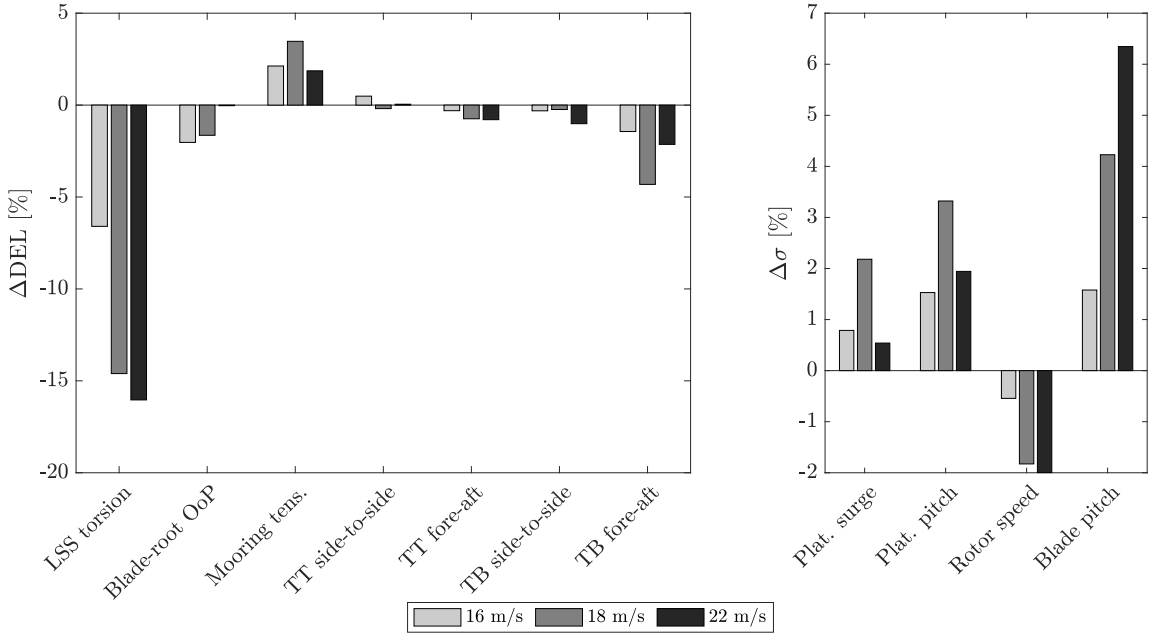

Figure 14. The damage equivalent load (DEL) and standard deviation (σ) with FBFF for three above-rated power production conditions. A negative Δ means a reduction with respect to feedback-only control. LSS stands for low-speed shaft, OoP for out-of-plane, TT for tower-top and TB for tower-base.

8 Conclusions

This paper investigated a model-inversion feedforward control strategy for the mitigation of wave disturbance in floating offshore wind turbines. A linear control-design model is utilized to carry out an MIMO analysis of the floating wind turbine. Collective-pitch is more effective than generator torque for rotor speed control in above-rated winds. Above the platform natural frequencies, wave equally affects rotor and platform motions, with a strength comparable to wind speed. Based on linear analysis, a model-inversion feedforward controller is designed for canceling the wave-induced rotor speed (and generator power) oscillations using collective-pitch. The feedforward controller is added to an industry-standard feedback controller. The performance improvement is demonstrated by means of linear analysis. A gain-scheduling algorithm is devised to improve

https://doi.org/10.5194/wes-2021-9
Preprint. Discussion started: 1 March 2021

the controller performance by adapting the feedforward action as the wind turbine operating condition changes. The control strategy is finally verified by means of time-domain simulations in a non-linear aero-servo-hydro-elastic model. It is found that feedforward control can reduce the standard deviation of rotor speed up to 2%. It also has a positive side effect on the damage-equivalent load of several wind turbine components: the shaft torsion is reduced of 15%, the tower-base fore-aft bending of 5%. Platform motions are however slightly increased and this is reflected into the mooring line loads.

The following suggestions should be considered in future work about wave-based control in floating wind turbines:

- the proposed feedforward controller is linear and compensates only for first-order wave loads. Recent numerical and experimental studies proved that second-order wave loads have a noticeable effect on the response of the floating wind turbine Roald et al. (2013). Thus, a first research suggestion is to investigate non-linear controllers and to include second-order hydrodynamics in the controller design;

- in the control-design model, rotor aerodynamics are modeled based on the quasi-steady theory. Thus, the controller obtained from the model does not account for unsteady aerodynamic effects, which may be significant for the response in the upper wave-frequency range Mancini et al. (2020). It is therefore suggested to develop a control-oriented model of the unsteady rotor aerodynamics and to include it in the control-design model, so to investigate how unsteadiness affects the response of the controlled FOWT.

- in the case at hand, the feedforward controller is designed to regulate rotor speed, and the reduction of fatigue loads is obtained as a positive side effect. As it has been shown, a large part of rotor speed oscillations is caused by wind turbulence; the wave disturbance drives platform motions and, consequently, it is cause of increased tower fatigue loads. It is therefore advisable to use the wave information to control the platform motions and use another controller, that also includes the wind measurement, to reduce rotor speed and power fluctuations;

- the wave prediction model may find application in several control-related tasks, which are not envisioned here. Waves drive the rigid-body motion of the floating platform, which in turn is likely to have an effect on the wind turbine wake. Wave prediction may be included in future floating wind farm control strategies;

- single-input single-output feedback controllers remain the default choice in floating wind turbines and advanced controllers are still far from reaching commercial projects. Tighter relationships between industry and academia are advisable to promote the adoption of advanced control strategies.

Author contributions. AF and MA developed the wave feedforward control methodology in all its aspects. MB and JWvW supervised the research activity mentoring AF and MA. Finally, AF prepared the manuscript of this article with contribution from all co-authors.

Competing interests. The authors declare that they have no conflict of interest.

https://doi.org/10.5194/wes-2021-9
Preprint. Discussion started: 1 March 2021

eawe european academy of wind energy
Open Access WIND ENERGY SCIENCE DISCUSSIONS

References

WAMIT User Manual - Version 7.0, http://www.wamit.com/manualupdate/history/V70_manual_old.pdf.

Al, M., Fontanella, A., van der Hoek, D., Liu, Y., Belloli, M., and van Wingerden, J. W.: Feedforward control for wave disturbance rejection on floating offshore wind turbines, Journal of Physics: Conference Series, 1618, 022 048, https://doi.org/10.1088/1742-6596/1618/2/022048, https://doi.org/10.1088%2F1742-6596%2F1618%2F2%2F022048, 2020.

Azcona, J., Vittori, F., Paulsen, U., Savenije, F., Kapogiannis, G., Karvelas, X., Manolas, D., Voutsinas, S., Amann, F., Faerron Guzman, R., and Lemmer, F.: Design Solutions for 10MW Floating Offshore Wind Turbines. Deliverable 4.37. INNWIND.EU., 2017.

Bak, C., Zahle, F., Bitsche, R., Taeseong, K., Yde, A., Henriksen, L. C., Hansen, M. H., Jose, J. P. A. A., Gaunaa, M., and Natarajan, A.: The DTU 10-MW Reference Wind Turbine, DTU Wind Energy Report, 2013.

Bayati, I., Belloli, M., Bernini, L., and Zasso, A.: A formulation for the unsteady aerodynamics of floating wind turbines, with focus on the global system dynamics, vol. 10, https://doi.org/10.1115/OMAE2017-61925, https://www.scopus.com/inward/record.uri?eid=2-s2.0-85019881350&doi=10.1115%2fOMAE2017-61925&partnerID=40&md5=925df27be7497b2239ac8b359fa7811a, 2017.

Dunne, F., Pao, L., Wright, A., Jonkman, B., and Kelley, N.: Combining Standard Feedback Controllers with Feedforward Blade Pitch Control for Load Mitigation in Wind Turbines, https://doi.org/10.2514/6.2010-250, https://arc.aiaa.org/doi/abs/10.2514/6.2010-250, a.

Dunne, F., Pao, L., Wright, A., Jonkman, B., Kelley, N., and Simley, E.: Adding Feedforward Blade Pitch Control for Load Mitigation in Wind Turbines: Non-Causal Series Expansion, Preview Control, and Optimized FIR Filter Methods, https://doi.org/10.2514/6.2011-819, https://arc.aiaa.org/doi/abs/10.2514/6.2011-819, b.

Dunne, F., Schlipf, D., Pao, L., Wright, A., Jonkman, B., Kelley, N., and Simley, E.: Comparison of Two Independent Lidar-Based Pitch Control Designs, https://doi.org/10.2514/6.2012-1151, https://arc.aiaa.org/doi/abs/10.2514/6.2012-1151, c.

Fontanella, A., Bayati, I., and Belloli, M.: Linear coupled model for floating wind turbine control, Wind Engineering, 42, 115–127, https://doi.org/10.1177/0309524X18756970, https://www.scopus.com/inward/record.uri?eid=2-s2.0-85044356122&doi=10.1177%2f0309524X18756970&partnerID=40&md5=892dd8a701a5fea8038c744de1a4ef42, 2018.

Fontanella, A., Al, M., van der Hoek, D., Liu, Y., van Wingerden, J., and Belloli, M.: A control-oriented wave-excited linear model for offshore floating wind turbines, Journal of Physics: Conference Series, 1618, 022 038, https://doi.org/10.1088/1742-6596/1618/2/022038, https://doi.org/10.1088%2F1742-6596%2F1618%2F2%2F022038, 2020.

Harris, M., Hand, M., and A., W.: Lidar for Turbine Control. Technical Report NREL/EL-500-39154, https://www.nrel.gov/docs/fy06osti/39154.pdf, 2006.

Janssen, R., Jansen, H., and Van Wingerden, J.-W.: A novel strategy for the identification of radiation force models, vol. 1A, https://doi.org/10.1115/OMAE2014-23504, https://www.scopus.com/inward/record.uri?eid=2-s2.0-84911362558&doi=10.1115%2fOMAE2014-23504&partnerID=40&md5=a6552b66881512877457abc68a42a4b4, 2014.

Jonkman, J. M. and Marshall, L. B.: FAST User's Guide. Technical Report NREL/EL-500-38230, https://nwtc.nrel.gov/system/files/FAST.pdf, 2005.

Jonkman, J. M., Wright, A. D., Hayman, G. J., and Robertson, A. N.: Full-System Linearization for Floating Offshore Wind Turbines in OpenFAST, https://doi.org/10.1115/IOWTC2018-1025, 2018.

Lackner, M. A.: Controlling Platform Motions and Reducing Blade Loads for Floating Wind Turbines, Wind Engineering, 33, 541–553, https://doi.org/10.1260/0309-524X.33.6.541, https://doi.org/10.1260/0309-524X.33.6.541, 2009.

https://doi.org/10.5194/wes-2021-9
Preprint. Discussion started: 1 March 2021

Laks, J., Pao, L., Wright, A., Kelley, N., and Jonkman, B.: Blade Pitch Control with Preview Wind Measurements, https://doi.org/10.2514/6.2010-251, https://arc.aiaa.org/doi/abs/10.2514/6.2010-251.

Larsen, T. and Hanson, T.: A method to avoid negative damped low frequent tower vibrations for a floating, pitch controlled wind turbine, vol. 75, https://doi.org/10.1088/1742-6596/75/1/012073, https://www.scopus.com/inward/record.uri?eid=2-s2.0-34548156706&doi=10.1088%2f1742-6596%2f75%2f1%2f012073&partnerID=40&md5=da0d731b888cd0eaf76d9406fbe321d6, 2007.

Lemmer, F., Raach, S., David, S., Faerron-Guzmá, R., and Cheng, P. W.: FAST model of the SWE-TripleSpar floating wind turbine platform for the DTU 10MW reference wind turbine, https://doi.org/10.18419/darus-514, https://doi.org/10.18419/darus-514, 2020.

Lemmer (ne Sandner), F., Yu, W., Schlipf, D., and Cheng, P. W.: Robust gain scheduling baseline controller for floating offshore wind turbines, Wind Energy, 23, 17–30, https://doi.org/10.1002/we.2408, https://onlinelibrary.wiley.com/doi/abs/10.1002/we.2408, 2020.

Levine, W.: The Control Handbook, 1996.

Mancini, S., Boorsma, K., Caboni, M., Cormier, M., Lutz, T., Schito, P., and Zasso, A.: Characterization of the unsteady aerodynamic response of a floating offshore wind turbine, https://doi.org/10.5194/wes-2020-94, 2020.

Naaijen, P. and Wijaya, A.: Phase resolved wave prediction from synthetic radar images, in: Proceedings of ASME 2014, 33rd International Conference on Offshore Mechanics and Arctic Engineering - OMAE, pp. 1–9, ASME, United States, https://doi.org/10.1115/OMAE2014-23470, 2014.

Newman, J. N.: Second-order, slowly-varying Forces on Vessels in Irregular Waves, 1974.

Perez, T. and Fossen, T.: A Matlab Toolbox for Parametric Identification of Radiation-Force Models of Ships and Offshore Structures, Modeling, Identification and Control, 30, https://doi.org/10.4173/mic.2009.1.1, 2009.

Reichert, K., Dannenberg, J., and van den Boom, H.: X-Band radar derived sea surface elevation maps as input to ship motion forecasting, in: OCEANS'10 IEEE SYDNEY, pp. 1–7, https://doi.org/10.1109/OCEANSSYD.2010.5603968, 2010.

Roald, L., Jonkman, J., Robertson, A., and Chokani, N.: The Effect of Second-order Hydrodynamics on Floating Offshore Wind Turbines, Energy Procedia, 35, 253 – 264, https://doi.org/https://doi.org/10.1016/j.egypro.2013.07.178, http://www.sciencedirect.com/science/article/pii/S1876610213012642, DeepWind'2013 – Selected papers from 10th Deep Sea Offshore Wind R&D Conference, Trondheim, Norway, 24 – 25 January 2013, 2013.

Schlipf, D., Schlipf, D. J., and Kühn, M.: Nonlinear model predictive control of wind turbines using LIDAR, Wind Energy, 16, 1107–1129, https://doi.org/10.1002/we.1533, https://onlinelibrary.wiley.com/doi/abs/10.1002/we.1533, 2013.

Schlipf, D., Simley, E., Lemmer, F., Pao, L., and Cheng, P. W.: Collective Pitch Feedforward Control of Floating Wind Turbines Using Lidar, Journal of Ocean and Wind Energy, 2, https://doi.org/10.17736/jowe.2015.arr04, 2015.

Skogestad, S. and Postlethwaite, I.: Multivariable feedback control: Analysis and Design, John Wiley, 2005.

van der Veen, G., Couchman, I., and Bowyer, R.: Control of floating wind turbines, in: 2012 American Control Conference (ACC), pp. 3148–3153, https://doi.org/10.1109/ACC.2012.6315120, 2012.

Yu Ma and Paul D. Sclavounos and John Cross-Whiter and Dhiraj Arora: Wave forecast and its application to the optimal control of offshore floating wind turbine for load mitigation, Renewable Energy, 128, 163 – 176, https://doi.org/https://doi.org/10.1016/j.renene.2018.05.059, http://www.sciencedirect.com/science/article/pii/S0960148118305809, 2018.

Ziemer, F. and Dittmer, J.: A system to monitor ocean wave fields, in: Proceedings of OCEANS'94, vol. 2, pp. II/28–II/31 vol.2, https://doi.org/10.1109/OCEANS.1994.364010, 1994.